Langmuir−Blodgett Films of Metal Complexes of 4-(10,12-Pentacosadiynamidomethyl)pyridine: A Structural Investigation

P. J. Werkman, R. H. Wieringa, E. J. Vorenkamp, and A. J. Schouten*

Department of Polymer Chemistry, University of Groningen, Nijenborgh 4, 9747 AG Groningen, The Netherlands

Received June 17, 1997. In Final Form: November 14, 1997

Complex formation between 4-(10,12-pentacosadiynamidomethyl)pyridine and metal ions in the subphase results in stable Langmuir monolayers up to surface pressures of 35 mN m^{-1}. Electron microscopy pictures show a flat monomer monolayer before polymerization and a polymer monolayer exhibiting a more striated structure after polymerization. Multilayers of the amphiphile can only be built up after complexation with metal ions. X-ray photoelectron spectroscopy (XPS) measurements definitely confirm the presence of metal ions in the multilayers, and the molar ratio between metal and amphiphile is derived from the spectra. These multilayers are further characterized by means of small-angle X-ray reflection measurements and Fourier transform infrared (FT-IR) spectroscopy, which show that the amphiphile has a large tilt angle (α) with respect to the surface normal. The multilayers are polymerized by means of UV irradiation, and UV−vis spectroscopy is used to study the polymerization process. The structural changes during polymerization are deduced from small-angle X-ray reflection measurements and FT-IR spectroscopy. In all cases, the bilayer spacing decreases during the polymerization process, whereas in some cases the regular plane of the all-*trans* conformation of the alkyl chains is converted to an irregular one containing gauche conformations. For multilayers built up from a $CuCl_2$-containing subphase, the whole distinct layer structure is destroyed during the polymerization process.

Introduction

The interaction of metal ions in the subphase with amphiphiles is well-known. The metal ions were mostly used to stabilize the monolayer,[1−3] for example, a monolayer of cadmium arachidate is much more stable than an arachidic acid monolayer alone, due to the cross-linking action of the Cd^{2+} ions, but other divalent cations, such as Pb^{2+}, Ca^{2+}, Ba^{2+}, etc., also have a stabilizing effect on the fatty acid monolayers as was already shown by Katherine Blodgett.[4,5] The interactions are of major importance for the manufacture of high-quality Langmuir−Blodgett (LB) films; even small amounts of cations enhance the stability of these fatty acid monolayers and condense them over a particular pH range characteristic for the metal ion dissolved in the subphase. The interaction of the metal ions with the acids depends largely on the physical and chemical properties of the metal ion. For instance, triple valent cations, like Fe^{3+} and Al^{3+}, in the subphase, tend to produce extremely rigid monolayer films with fatty acids that can hardly be transferred onto substrates.[1]

Nowadays there is a growing interest in making functional LB films in which the metal ions introduce special semiconducting, magnetic, or quantum physical properties into these multilayer films,[1,6,7] and these films have potential applications as sensors, for chemically modification of electrodes, in catalytic systems, and in microelectronic devices.

In principle, the metal ions can be incorporated into the monolayer film in two ways. First, by means of salt or complex formation by the amphiphile from the subphase wherein the metal ions are dissolved, and second the metals could be bound to the amphiphile before spreading the formed salt or the metal complex at the air−water interface.[8,9] Dithiooxamides,[10,11] pyridines,[12,13] porphyrines,[14] and phthalocyanines[15,16] are often used as ligands for complex formation with metal ions. When crown ethers and imidazoles are used as ligand units in amphiphiles, even at very low subphase concentrations (10^{-6} M), metal ions are incorporated into the floating monolayer at the air−water interface, as was shown by Lednev and Petty[17] and van Esch et al.[18] Also, metal ions could be incorporated into floating polymer monolayers with an amphiphilic character that have ligand groups such as pyridine,[19]

(1) Roberts, G., Ed.; *Langmuir−Blodgett Films*; Plenum: New York and London, 1990.
(2) Ulman, A. *An Introduction to Ultrathin Organic Films: From Langmuir−Blodgett to Self-Assembly*; Academic: San Diego and London, 1991.
(3) Linden, D. J. M.; Peltonen, J. P.; Rosenholm, J. B. *Langmuir* **1994**, *10*, 1592.
(4) Blodgett, K. B. *J. Am. Chem. Soc.* **1935**, *57*, 1007.
(5) Blodgett, K. B. Langmuir, I. *Phys. Rev.* **1937**, *51*, 964.
(6) Miyashita, T. *Prog. Polym. Sci.* **1993**, *18*, 263.
(7) Swalen, J. D.; Allara, D. L.; Andrade, J. D.; Chandross, E. A.; Garoff, G.; Israelachvili, J.; McCarthy, T. J.; Murray, R.; Pease, R. F.; Rabolt, J. F.; Wynne, K. J.; Yu, H. *Langmuir* **1987**, *3*, 932.
(8) Wang, K. Z.; Huang, C. H.; Zhou, D. J.; Xu, G. X.; Xu, Y.; Liu, Y. Q.; Zhu, D. B.; Zhao, X. S.; Xie, X. M. *Solid State Comm.* **1995**, *93*(*3*), 189.
(9) Bonsoni, F.; Lely, F.; Ricciardi, G.; Romanelli, M.; Martini, G. *Langmuir* **1993**, *9*, 268.
(10) Suzuki, A.; Ohkawa, K.; Kanda, S.; Emoto, M.; Watari, S. *Bull. Chem. Soc. Jpn.* **1975**, *48*(*10*), 2634.
(11) Sasakawa, K.; Iwata, S. *Annu. Rep. Res. Reactor Inst. Kyoto University* **1984**, *17*, 146.
(12) Caminati, G.; Margheri, E.; Gabrielli, G. *Thin Solid Films* **1994**, *244*, 905.
(13) Caminati, G.; Margheri, E.; Gabrielli, G. *Prog. Colloid Polym. Sci.* **1994**, *97*, 12.
(14) Satori, E.; Fontana, M. P.; Costa, M.; Dalcanale, E.; Paganuzzi, V. *Thin Solid Films* **1996**, *284−285*, 204.
(15) Gobernado-Mitre, M.; Aroca, R. *Langmuir* **1993**, *9*, 2185.
(16) Kalvoda, L.; Brynda, E. *Thin Solid Films* **1993**, *232*, 120.
(17) Lednev, I. K.; Petty, M. C. *Adv. Mater.* **1996**, *8*(*8*), 615.
(18) van Esch, J. H.; Nolte, R. J. M.; Ringsdorf, H.; Wildburg, G. *Langmuir* **1994**, *10*, 1955.
(19) Nagel, J.; Oertel, U. *Polymer* **1995**, *36*(*2*), 381.

S0743-7463(97)00642-2 CCC: $15.00
Published on Web 03/13/1998

Chart 1

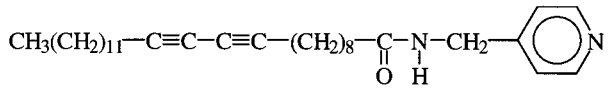

bipyridine,[20] or crown ethers.[17]

As we have shown in a previous publication,[21] the amphiphile 4-(10,12-pentacosadiynamidomethyl)pyridine (Chart 1) can form coordination complexes with Cu(II) at the air−water interface when the copper ions are dissolved in the subphase.

We showed that the amount of complexation could easily be tuned by choosing the desired complexation conditions. This amphiphile contains a diacetylene functionality in the aliphatic tail, which can be polymerized upon UV irradiation, resulting in a polymer multilayer with enhanced thermal and mechanical stability. In addition to these favorable mechanical properties, polydiacetylenes are highly conjugated, linear polymers, that exhibit thermo- and solvatochromism, and semiconducting as well as strong third-order nonlinear optical properties.[22−25] In principle, polydiacetylenes might find applications as ultrathin resins or protective coatings, or in integrated optical devices.

In the present work, the morphology of the monolayer before and after exposure to UV light was studied by electron microscopy. Furthermore, we show that multilayers could only be built up of monomer monolayers when the subphase contained Cu^{2+} or Cd^{2+} cations. The structure of these multilayers was deduced from X-ray photoelectron spectroscopy (XPS), small-angle X-ray reflection, and Fourier transform infrared (FT-IR) measurements, which revealed major changes when the cation or counterions dissolved in the subphase were changed. Polymerization of the multilayers was followed by UV−vis spectroscopy. The structural changes during the polymerization process were studied by small-angle X-ray reflection and FT-IR measurements. From these studies we conclude that the layer structure is preserved well with one exception; that is, in the case of multilayers built up from a $CuCl_2$-containing subphase, the layer structure is destroyed during exposure to UV light.

Experimental Section

Materials. 10,12-Pentacosadiynoic acid (Hüls-Petrarch, > 99%) was reacted with thionyl chloride (Merck, > 99%) to obtain the corresponding acid chloride. The amide derivative, 4-(10,12-pentacosadiynamidomethyl)pyridine, was obtained in good yields (70%) by reaction of 4-(aminomethyl)pyridine (Acros, 98%) with the acid chloride in dry benzene (Merck p.a.) under nitrogen atmosphere. Triethylamine (Merck, > 99%), distilled under nitrogen atmosphere from CaH_2, was added as a HCl scavenger. The crude product was purified by a two-fold crystallization from acetone (Merck p.a.). Elemental analysis: Calc. for $C_{31}H_{48}N_2O$: C 80.17; H 10.34; N 6.03. Found: C 80.05; H 10.33; N 6.03. IR: ν (cm^{-1}) 3294 (ν NH), 2919 (ν_a CH_2), 2849 (ν_s CH_2), 1644 (amide I), 1600 (ν C═N, aromatic ring), 1561 (ν C═C, aromatic ring), 1545 (amide II), 1465 (δ CH_2). ^{1}H NMR (200 MHz): δ 0.87 (t, 3H), 1.24−1.31 (br, 26H), 1.46 (m, 4 H), 1.66 (m, 2H), 2.19 (t, 2H), 2.26 (t, 4H), 4.44 (d, 2H), 6.00 (s, 1H), 7.17 (d, 2H), 8.53 (d, 2H). T_m = 76 °C, T_c = 51 °C.

$Cu(ClO_4)_2$ (Acros, 98%), $CuCl_2$ (Merck, ≥ 99%), and $CdBr_2$ (Merck, 98%) were used without further purification. A 5 mM $Cu(ClO_4)_2$ subphase has a pH of 4.9 and a 5 mM $CuCl_2$ subphase has a pH of 4.9. Increasing the Cu(II) ion concentration to 10 mM results in a subphase pH of ∼4.7, irrespective of the counterion used. The subphase cannot be made much more basic because when the pH values of the subphase are 6.00 or higher, a $Cu(OH)_2$ precipitate is formed.

Langmuir−Blodgett (LB) Films. The monolayer properties were studied by measuring pressure−area isotherms using a commercially available computer controlled Lauda-Filmbalance (FW 2). The water used for the subphase was purified by a Milli-Q filtration system preceded by a reversed osmosis filtration (Elgastat spectrum SC30). The amphiphile was dissolved in chloroform (Merck, spectroscopic quality), with a concentration of 0.1 wt %, and the isotherms were recorded with a compression speed of 10 $Å^2$ (molecule min)$^{-1}$ at different temperatures. Glass slides, quartz slides, and silicon wafers, used as substrates, were subsequently treated with a mixture of H_2O_2 (30%)/NH_3 (25%)/H_2O (1:1:5, v/v) for 30 min at 60 °C; ultrasonically treated with a mixture of HCl (37%)/H_2O (1:6, v/v) for 15 min; washed several times with Milli-Q water; again ultrasonically cleaned with methanol (Merck p.a.), methanol/chloroform (3:1, v/v) mixture, and chloroform (Merck p.a.) for 15 min; and finally stored in methanol. Before use, the substrates were hydrophobized by treating them with a mixture of chloroform and hexamethyldisilazane (Acros, 98%; 4:1, v/v) at 50 °C, and finally rinsed with chloroform. Gold substrates were obtained by sputtering a 250-nm-thick gold layer onto the cleaned glass slides. A dipping speed of 2 mm min^{-1} was used for both the down and upstroke transfer.

Polymerization. The multilayers were polymerized using a Rayonette Photochemical Reactor, which contained UV lamps (254 nm, 24 W). The polymerization was carried out under an argon atmosphere. The distance of the lamps to the center of the photochemical reactor was 12 cm. This distance corresponds to an intensity of ∼0.2 W cm^2. After a constant flow of argon for 40 min, the polymerization of the monolayer at the air−water interface was carried out at a surface pressure of 30 mN m^{-1}, using a small UV lamp (254 nm, 3 W) at a 5-cm distance, which corresponds to an intensity of ∼0.003 W cm^2.

Infrared (IR) Measurements. The transmission IR measurements were carried out with a Mattson Galaxy 6021, and the grazing incidence reflection measurements were performed on a Bruker IFS-88 FT-IR spectrophotometer equipped with a Spectra-Tech Inc. fixed-angle (80°) GIR accessory. Spectra were recorded with a 4 cm^{-1} resolution.

The IR spectra at elevated temperatures were recorded with the Mattson Galaxy 6021 equipped with a custom-made AABSPEC multi-mode FT-IR cell (model #95S−E) with a transmission and GIR probe (80°).

UV−vis Spectroscopy. UV−vis absorption spectra of the multilayers on glass slides were recorded on a SLM-Aminco 300 diode-array UV−vis spectrophotometer.

XPS Measurements. The XPS spectra were obtained with a X-Probe 300 of Surface Sciences Instruments spectrometer with monochromated Al Kα radiation with energy of 1486.6 eV. Measurements were carried out with a resolution of 1.8 and 0.4 eV for the overall and narrow scan, respectively, and a takeoff angle of 45°. Binding energy values are referred to the aliphatic carbon 1S line, taken as 287.0 eV.

Small-Angle X-ray Reflection Measurements. Small-angle X-ray reflection measurements were performed with a Philips PW1830 generator and a Philips PW1820 diffractometer in a $\theta/2\theta$ geometry, using Cu Kα radiation (λ = 1.542 Å).

Electron Microscopy. Samples for transmission electron microscopy (TEM) were prepared by transferring the monolayer, stabilized at a surface pressure of 30 mN m^{-1}, onto a carbon-coated copper grid, which had been made hydrophilic by glow discharge in air under reduced pressure, by a manual horizontal lifting method. The samples were Pt-shadowed at an angle of 20°. TEM micrographs were recorded with a Philips EM 300 using a acceleration voltage of 80 kV at a magnification of 10 000×.

(20) Miyashita, T.; Saito, S.; Matsuda, M. *Chem. Lett.* **1991**, 859.
(21) Werkman, P. J.; Schouten, A. J. *Thin Solid Films* **1996**, *284−285*, 24.
(22) Tieke, B.; Graf, H.-J.; Wegner, G.; Naegele, B.; Ringsdorf, H.; Banerjie, A.; Day, D.; Lando, J. B. *Colloid Polym. Sci.* **1977**, *255*, 521.
(23) Burzynski, R.; Prasad, P.; Biegajski, J.; Cadenhead, D. A. *Macromolecules* **1986**, *19*, 1059.
(24) Bubeck, C. *Thin Solid Films* **1980**, *160*, 1.
(25) Göbel, H. D. Fluoreszenze-, Röntgen-, and Elektronenoptische Untersuchung von Phasenverhalten, Mikrostruktur und Polymerisation Monomolekulare Schichten aus vernetzbaren Lipiden. Thesis, Technische Universität München, 1989.

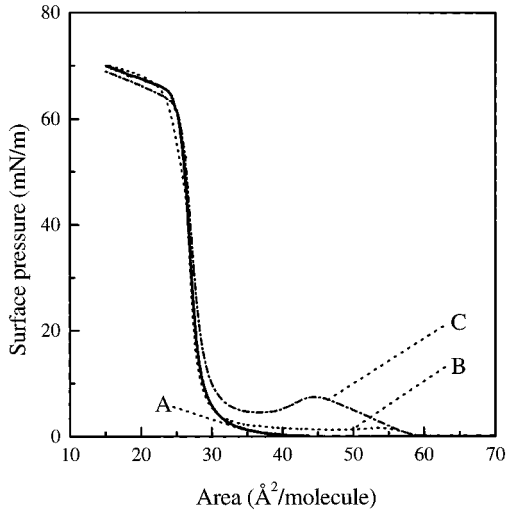

Figure 1. Surface pressure-area isotherms of the amphiphile at 18.7 °C on an aqueous subphase (A) and on a subphase containing 5 mM $CuCl_2$ (B) and 5 mM $Cu(ClO_4)_2$ (C).

Results and Discussion

Monolayer. Figure 1 clearly shows the effect of the addition of Cu(II) ions with different counterions (Cl^- and ClO_4^-). On an aqueous subphase, the compound forms a condensed (C) monolayer film at 18.7 °C. When the subphase contains Cu(II) ions, a liquid-expanded (LE) to liquid-condensed (LC) phase transition can be observed, which indicates that complexation has taken place at the air−water interface. Upon complexation, a charged monolayer is formed in which the amphiphiles start to repel each other resulting in an expanded monolayer.[21] When ClO_4^- was used as counterion, the surface pressure at which the phase transition (Π_c) from LE to LC phase appears was higher than in the case when Cl^- was used as a counterion. This result indicates that when ClO_4^- is used as a counterion, a more complete complexation takes place, as has already been pointed out in our earlier publication.[21]

With or without metal ions in the subphase, these monolayers could be stabilized at surface pressures up to 35 mN m^{-1} with subphase temperatures up to 25 °C and form very stable monolayers within 30 min at a surface area of ~27 $Å^2$ $molecule^{-1}$.

These monolayers could be polymerized at the air−water interface after 40 min of a constant flow of argon, by means of a small UV lamp (254 nm, 1.6 W) for 2 min, resulting in a small contraction of the monolayer. The polymerized monolayer was very brittle and appeared blue, as could be seen by the naked eye. Figure 2 shows the transmission electron micrographs of the monomer (Figure 2A) and polymer (Figure 2B) monolayers picked up at a surface pressure of 30 mN m^{-1} on a 5 mM $Cu(ClO_4)_2$ subphase. The monomer monolayer appeared to be very smooth; the fold on the left upper side of Figure 2A, is formed during the preparation of the sample, and will therefore not be present in the monolayer at the air−water interface. The polymer monolayer has a striated texture, which is often seen for polydiacetylene monolayers (Sarkar et al.,[26] Putman et al.[27]). The crack on the upper left side of Figure 2B, again, was formed during the preparation. This crack was exactly formed on the border of two crystals as can be seen from direction of the striations, indicating the chain direction of the polymer backbone.[26] From Figure 2B it is possible to estimate the thickness of one polymer monolayer by measuring the length of the shadow. From the equation $h = l \times \tan \alpha$, in which h is the thickness of the monolayer, l is the length of the shadow, and α is the angle at which the samples were Pt-shadowed, the monolayer thickness can be calculated. The estimated thickness is in the order of 33 ± 8 Å.

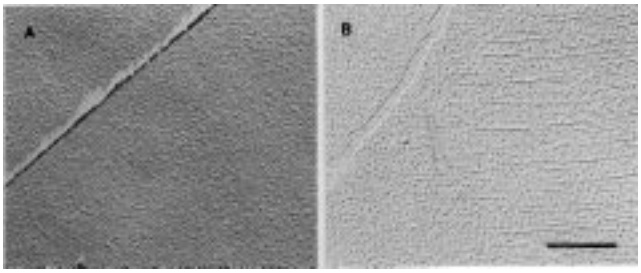

Figure 2. Transmission electron micrographs of transferred monomer and polymer monolayers at a subphase temperature of 19 °C and a surface pressure of 30 mN m^{-1}. The polymer monolayer was formed after UV irradiation of the monomer monolayer at the air−water interface for 2 min under argon atmosphere. The scale bar corresponds to 0.2 μm.

Table 1. Samples Used in This Study[a,b]

sample	substrate	subphase	surface pressure (mN m^{-1})
A	silicon	5 mM $Cu(ClO_4)_2$	30
B	glass	5 mM $Cu(ClO_4)_2$	30
C	Au with 3 layers of cadmium arachidate	5 mM $Cu(ClO_4)_2$	30
D	Au with 3 layers of cadmium arachidate	1 mM $Cu(ClO_4)_2$	30
E	silicon	5 mM $CuCl_2$	30
F	silicon	5 mM $CdBr_2$	19

[a] All samples consisted of 16 layers of the amphiphile. [b] Subphase temperature is 19 °C.

Multilayer Formation. Transfer experiments were carried out at surface pressures between 18 and 30 mN m^{-1} and with a subphase temperature of 19 °C. The polymer monolayer could not be transferred onto solid substrates because it is too brittle and too stiff. When the monolayers were deposited onto a solid substrate (glass, quartz, gold, or silicon), Z-type transfer was observed, with transfer ratios of 0.0 on the downstroke and 1.0 on the upstroke, irrespective of the counterions used (Cl^-, ClO_4^-, or Br^-).

In Table 1 the different samples used in this study are listed.

Cu(II)-Containing Multilayers. The XPS measurements were performed on these multilayers to confirm the presence of metal ions in these samples and to give quantitative information about the amount of metal ions incorporated into the LB films. The XPS spectrum of a multilayer built up from a 5 mM $Cu(ClO_4)_2$ subphase (Sample A) is shown in Figure 3. We can clearly see the copper peaks, but it appeared to be a mixture of Cu(II) (peaks at 936.5 and 956.5 eV with the associated satellites) and Cu(I) (peaks at 933.5 and 954.0 eV). This result is somewhat surprising because we only expected Cu(II) in the multilayers and no reduction to Cu(I). So, we studied the behavior of these multilayers inside the XPS spectrometer more closely. Upon longer exposure of the multilayer to soft X-rays, the Cu(I) peaks increased in time whereas the Cu(II) peaks decreased in intensity; also the satellites associated with Cu(II) disappeared. Finally, after 20 h of exposure to X-rays, almost all the Cu(II) is

(26) Sarkar, M.; Lando, J. B. *Thin Solid Films* **1983**, *99*, 119.
(27) Putman, C. A. J.; Hansma, H. G.; Gaub, H. E.; Hansma, P. K. *Langmuir* **1992**, *8*, 3014.

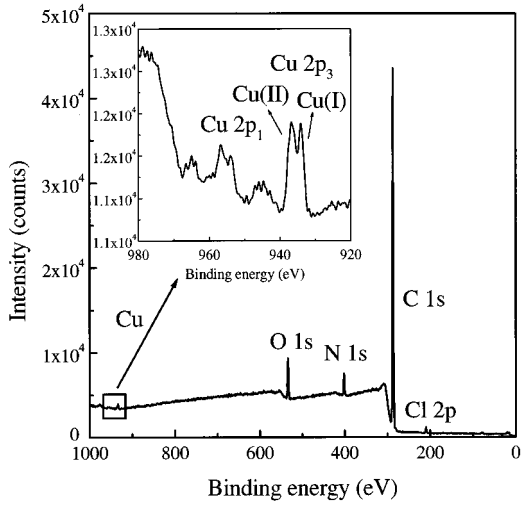

Figure 3. XPS spectrum of 16 layers of amphiphile, transferred from a $Cu(ClO_4)_2$ subphase at 19 °C and 30 mN m^{-1} on silicon (sample A).

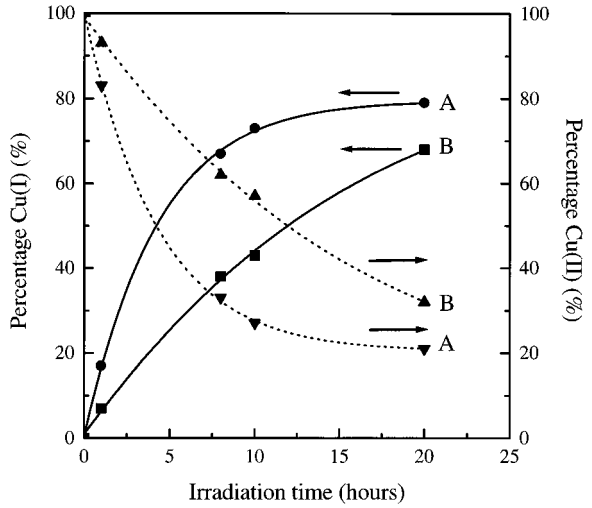

Figure 4. Percentage of Cu(I), calculated by the formula: [Cu(I) $2p_3$/(Cu(I) $2p_3$ + Cu(II) $2p_3$)] × 100%, at different irradiation times for Cu(II)-containing multilayers, built up from a 5 mM $Cu(ClO_4)_2$ (A, sample A) and 5 mM $CuCl_2$ (B, sample E) subphase at 19 °C at 30 mN m^{-1} on silicon. In determining the amount of Cu(II), the integrated area of the satellite was also taken into account, and the deconvolutions were performed by a best-fit Gaussian computer program.

reduced to Cu(I). In Figure 4 the Cu (II) and Cu(I) fraction is plotted as function of the exposure time to the soft X-rays in the XPS apparatus. It can clearly be seen that the fraction of Cu(I) increases at longer irradiation time and the Cu(II) ions are reduced. This phenomena has been described before for Cu^{2+} and some other metal ions (like Cr^{6+} and Fe^{3+}) in the literature.[28−33] This reduction is mainly caused by secondary electrons. When the multilayers were built up from a 5 mM $CuCl_2$ subphase, it could be seen that the initial X-ray-induced reduction of Cu(II) proceeds much slower than when ClO_4- was used as a counterion (Figure 4, curve B). After 1 h of exposure to X-rays, only a weak shoulder of Cu(I) can be seen in the case of Cl^--containing multilayers (~7%), whereas in the case of ClO_4^--containing multilayers, there is already a pronounced amount of Cu(I) present after 1 h of exposure to the soft X-rays. This lower reduction rate of the Cu(II) ions is probably caused by the difference in packing of multilayers which contain Cl^- or ClO_4^- as counterion. Probably, the multilayers that contain Cl^- as counterion are more dense than the multilayers that contain ClO_4^- as a counterion, causing slower reduction of the Cu(II) ions upon exposure to soft X-rays. This situation was also the case for the Cu(II) reduction inside α- and γ-zirconium phosphates,[33] which are layered compounds that differ in structure and packing sequence of layers, resulting in a different reduction rate of Cu(II) during the XPS experiments. In α-zirconium phosphate (which has the less dense structure of the two zirconium phosphates), the Cu(II) ions are reduced much faster than in γ-zirconium phosphate. When we used the floodgun for compensation of charging effects, immediately a total reduction of Cu(II) could be observed for multilayers that contain ClO_4^- as counterions, whereas with Cl^- as counterion the reduction still appeared very slow.

Table 2. The Ratio N:Cu of the Multilayers, Calculated from the XPS Spectra, As a Function of the $Cu(ClO_4)_2$ Concentration in the Subphase[a]

$[Cu(ClO_4)_2]$ (mM)	ratio N:Cu
10	4.2
5	4.7
1	17.2
0.5	25.8

[a] For all multilayers the ratio of Cu:Cl was 1:2.

The amount of Cu(II) ions incorporated in the multilayers can easily be varied by changing the subphase concentration of Cu(II), as can be seen in Table 2.

Stable monolayers can be formed on a $Cu(ClO_4)_2$-containing subphase up to concentrations of 10 mM. When the subphase contained >10 mM $Cu(ClO_4)_2$, stable monolayers cannot be formed anymore, probably because too many Cu(II) ions are coordinated to the monolayer, forming a heavily charged monolayer, and on compression, molecules probably are forced to dissolve into the subphase.

So, the maximum amount of Cu(II) ions in the multilayers [built up from a 10 mM $Cu(ClO_4)_2$-containing subphase] with ClO_4^- as counterion was ~1 Cu(II) ion to 2 amphiphiles, because each amphiphile contains 2 nitrogen atoms. When the subphase contained 5 mM $CuCl_2$, the multilayer contained ~1 Cu(II) ion to 3 amphiphiles. So, the ClO_4^- counterion causes a better complexation in the monolayer to occur, as was already discussed in a former publication.[21]

In Figure 5, the grazing incidence reflection (GIR) spectra of samples C and D are shown. The peak at 1621 cm^{-1} corresponds to the ν_{C-N} of the pyridine moiety coordinated to the metal, and the 1600 peak corresponds to ν_{C-N} of a free pyridine ring.[34,35] Clearly, sample D contains relative high amounts of noncoordinated pyridine ligands. The coordinated and noncoordinated pyridine rings most probably have the same orientation because the bands corresponding to both vibrations appear strongly in the GIR spectrum, but can hardly be seen in the transmission IR spectrum. From the XPS experiments it can be calculated that multilayers that were built up from

(28) Wallbank, B.; Johnson, C. E.; Main, I. G. *J. Electron Spectrosc.* **1974**, *4*, 263.
(29) Gilp, J. F.; Main, I. G. *J. Electron Spectrosc.* **1975**, *6*, 397.
(30) Angelis, B. A. *J. Electron Spectrosc.* **1976**, *9*, 81.
(31) Schön, G. *Surf. Sci.* **1973**, *35*, 96.
(32) Copperthwaite, R. G. *Surf. Interface Anal.* **1980**, *2(1)*, 17.
(33) Martella, G.; Puglisi, O.; Pignataro, S.; Alberti, G.; Costantino, U. *Chem. Phys. Lett.* **1982**, *89(4)*, 333.
(34) Ruokolainen, J.; Tanner, J.; ten Brinke, G.; Ikkala, O.; Torkkeli, M.; Serimaa, R. *Macromolecules* **1995**, *28*, 7779.
(35) Ruokolainen, J.; ten Brinke, G.; Ikkala, O.; Torkkeli, M.; Serimaa, R. *Macromolecules* **1996**, *29*, 3409.

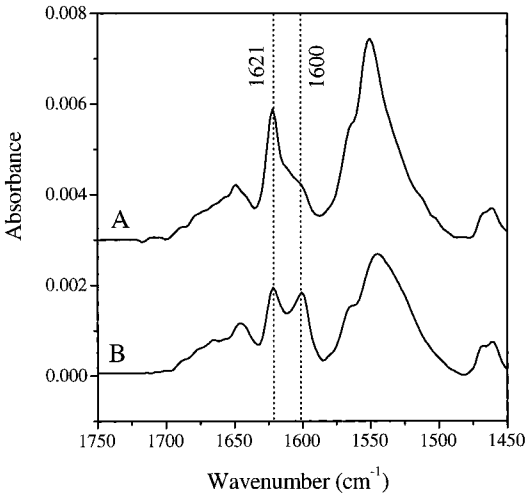

Figure 5. GIR infrared spectra of LB films consisting of 16 layers of the amphiphile on a gold-coated glass with three layers of cadmium arachidate, built up from a 5 mM (A, sample C) and 1 mM (B, sample D) $Cu(ClO_4)_2$ subphase at 19 °C and 30 mN m^{-1}.

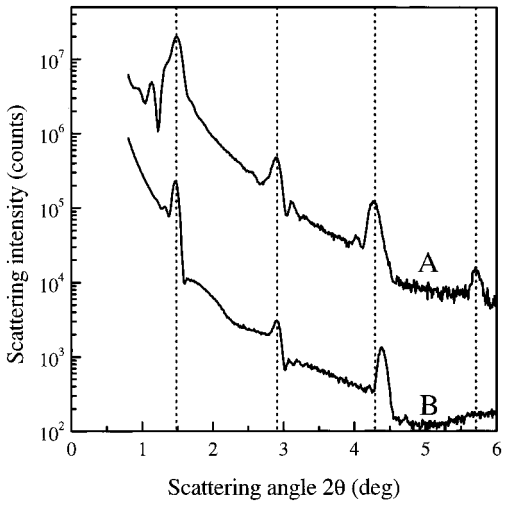

Figure 6. Small-angle X-ray reflection curves of 16 layers of the amphiphile built up from (A, sample A) 5 mM $Cu(ClO_4)_2$ and (B, sample E) 5 mM $CuCl_2$ subphase at 19 °C and 30 mN m^{-1} on silicon.

a 1 mM $Cu(ClO_4)_2$ subphase contain 1 Cu(II) ion on ~8.5 amphiphiles (each amphiphile having two nitrogens). Therefore, we assume that the multilayer built up from a 1 mM $Cu(ClO_4)_2$ subphase (sample D) consists of CuL_4 complexes (L: amphiphile) and free amphiphiles in the ratio CuL_4:4L because in the GIR spectrum of this multilayer, the peaks of the coordinated and noncoordinated pyridine ring have almost the same intensity.

The following equations can be considered for complexation of the amphiphile with metal ions.

$$L + M \leftrightarrow LM \quad (1)$$

$$L + ML \leftrightarrow ML_2 \quad (2)$$

$$L + ML_2 \leftrightarrow ML_3 \quad (3)$$

$$L + ML_3 \leftrightarrow ML_4 \quad (4)$$

$$nL + M \leftrightarrow ML_n \quad (5)$$

At high Cu(II) concentrations (> 10 mM $Cu(ClO_4)_2$) the equilibrium is shifted to the copper rich side, forming CuL complexes. This way, a heavily charged monolayer is formed that is not stable. At lower Cu(II) concentrations [10 and 5 mM $Cu(ClO_4)_2$], the relative amount of ligands (L) at the air−water interface is increased, so the equilibrium is shifted and CuL_2 complexes are formed, which is also indicated by the GIR measurements (Figure 5) in combination with the XPS measurements. At even lower concentration [1 mM $Cu(ClO_4)_2$ or lower] the equilibrium is totally shifted to the copper deficient side, forming CuL_4 complexes in a matrix of uncoordinated ligands. The composition of the formed complexes at the air−water interface may differ from the structure of the complexes found in the LB films, although the stoichiometry of the complexes will be the same because during the preparation of the multilayers, the structure of the multilayers is rearranged, as will be discussed in the next paragraph. This rearrangement of the multilayer structure may induce the formation of complexes that have a different structure than the complexes formed at the air−water interface.

To establish whether the formed multilayers had a distinct layer structure, small-angle X-ray reflection measurements were performed. The small-angle reflection X-ray patterns of the samples A and E are shown in Figure 6B, respectively. A regular layer pattern was observed for these Cu(II) ion-containing multilayers, with Bragg peaks representing layer spacings of 59.2 and 60.0 Å for the multilayers built up from 5 mM $Cu(ClO_4)_2$ and $CuCl_2$ subphases, respectively. The amphiphile, in fully stretched conformation, has a length of ~36.5 Å, so the layer spacings found must represent a bilayer spacing. Because these multilayers were built up by means of Z-type transfer, we expected a monolayer spacing between 30 and 37 Å. So, a rearrangement to a Y-type structure must have occurred in which the amphiphiles have a large tilt angle with respect to the surface normal, because for a perpendicular orientation of the amphiphiles to the substrate surface, a bilayer spacing of ~73 Å should have been found. The rearrangement of a Z-type structure in to a Y-type structure is a well-known phenomenon for low molecular weight amphiphiles.[1,36−39] The Y-type structure is the thermodynamically most stable structure, with the hydrophobic aliphatic tails and the hydrophilic headgroups facing each other.

To get more information on the orientation of amphiphiles in the LB films, transmission IR spectra (electrical field vector parallel to the substrate surface, so all individual group vibrations with transition dipole moment components parallel to the substrate surface will absorb maximally in this mode) and GIR IR spectra (electrical field vector perpendicular to the substrate surface, so all individual group vibrations with transition dipole moment components perpendicular to the substrate surface will absorb maximally in this mode) were recorded. In Figure 7 the different spectra can be seen for a multilayer built up from a 5 mM $Cu(ClO_4)_2$ subphase and the mode assignments are presented in Table 3.

To scale the bulk, transmission, and GIR spectra in a proper way, transmission and GIR spectra were also recorded at 60 °C. At this elevated temperature, the side chains are molten and all preferred orientation is lost. Also, a bulk spectrum of the amphiphile powdered in KBr was recorded at 80 °C, at this temperature the amphiphile

(36) Stephens, J. F. *J. Colloid Interface Sci.* **1972**, *38*, 557.
(37) Honig, E. *J. Colloid Interface Sci.* **1973**, *43*, 66.
(38) Honig, E. P.; Hengst, J. H.; den Engelsen, D. *J. Colloid Interface Sci.* **1973**, *45*, 92.
(39) Flanagan, M. T. *Thin Solid Films* **1983**, *99*, 133.

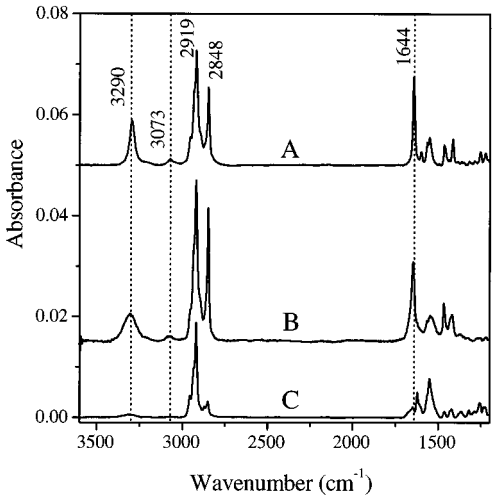

Figure 7. Infrared spectra of the amphiphile: (A) powdered in KBr (scale factor: 0.0395×); (B) transmission; (C) GIR (scale factor: 0.432×). In the case of GIR, 16 layers were transferred onto a gold-coated glass slide from a 5 mM $Cu(ClO_4)_2$ subphase (sample C), and in the case of transmission, 16 layers were transferred onto silicon at a subphase concentration of 5 mM $Cu(ClO_4)_2$ (sample A). In both cases, the subphase temperature was 19 °C and the surface pressure was 30 mN m^{-1}.

Table 3. The IR Band Assignments[a]

wavenumber (cm^{-1})	assignment	transition dipole moment, M
3301	ν (N−H)	|| N−H bond
2953	ν_a (CH_3)	⊥ C−CH_3
2920	ν_a (CH_2)	⊥ C−C−C chain plane
2871	ν_s (CH_3)	|| C−CH_3
2850	ν_s (CH_2)	|| H−C−H plane, bisecting HCH angle
1645	Amide I	|| C═O bond
1621	ν (C═N_{ar})	|| ring
1565	ν (C═C_{ar})	|| ring
1547	Amide II	⊥ C═O bond
1468	δ (CH_2)	|| H−C−H plane, bisecting HCH angle

[a] From refs 34, 35, 40−43.

is in the molten state. All these spectra were scaled in such a way that the vibrations in the CH stretching vibration region have the same intensity as in the transmission spectrum of sample A at 60 °C. These scaling factors were used for the bulk and GIR spectra at room temperature in Figure 7.

For the GIR measurements, gold substrates were used on which three layers of cadmium arachidate were deposited on the sample and reference side, so the three cadmium arachidate layers make no contribution to the GIR spectrum. Sixteen monolayers were deposited on top of these three layers of cadmium arachidate. Furthermore, a GIR spectrum was recorded when gold substrates were used on which three layers of poly((*S*)-1-acetoxymethylethylisocyanide) (reference and sample side) on top of which 16 monolayers of the amphiphile on a 5 mM $Cu(ClO_4)_2$ subphase were transferred. This spectrum was identical to the GIR spectra of Figure 7, which indicates that the three cadmium arachidate layers probably do not influence the structure of the LB film on top of these layers, which allows proper comparison of the transmission and reflection spectra.

In the bulk spectrum of the amphiphile, powdered in KBr, the individual groups have no preferred orientation. In the transmission spectrum (Figure 7B) we can clearly see the N−H (3301 cm^{-1}) and amide I (1645 cm^{-1}), whereas these absorption bands are nearly absent in the GIR spectrum. The integrated area of the amide I peak of the transmission spectrum is 1.5 times larger than the amide I peak of the bulk spectrum. The amide II (1545 cm^{-1}) vibration, on the contrary, is strongly present in the GIR mode and very weak in the transmission spectrum. From this result we conclude that the amide groups are oriented parallel to the substrate surface. Furthermore, the pyridine group vibration at 1621 cm^{-1} is strongly absorbing in the GIR spectrum and only weakly in the transmission spectrum; so, the pyridine group is oriented with a small angle with respect to the surface normal. Also, in the absorption region of the aliphatic tail vibrations, major differences could be observed. It can be seen that the intensities of the bands at 2919 (ν_a CH_2) and 2850 cm^{-1} (ν_s CH_2) differ tremendously in intensity comparing the transmission and GIR spectra. The asymmetric stretch vibrations of the methylene is absorbing strongly in the GIR spectrum, whereas the symmetric stretch vibration absorptions can hardly be seen. Both vibration absorptions are present in the transmission spectrum. These differences in intensity of the ν_a (CH_2) and ν_s (CH_2) between the GIR and transmission spectra are usually not observed when an all-*trans* CH_2 chain is oriented with an angle, α, with respect to the surface normal[40−45] and the C−C−C plane in the all-*trans* alkyl chain can take on any orientation around the chain axis. So, in the normal case, the intensities of ν_a (CH_2) and ν_s (CH_2) in the GIR or transmission spectrum depend only on the tilt angle, α, and the ratio of their intensities does not change significantly between these two spectrum measurement methods.

In the literature,[40,46−49] several reports have been published in which comparable changes in intensities of ν_a (CH_2) and ν_s (CH_2) have been described. Those results have been explained by assuming a special packing of the alkyl chains. Nuzzo et al.[46] and Evans et al.[47] interpreted their results as due to a close packing of the CH_2 chains in a triclinic lattice instead of an orthorhombic. This close packing was supposed to be induced by strong dipoles of the sulfone groups incorporated in the alkyl chain. In that way, the all-*trans* C−C−C plane had a preferred orientation in which this plane was oriented at a certain angle with respect to the substrate surface and could not take on all possible orientations around the chain director. This result was also found by Walsh and Lando[50] for alternating multilayers of diacetylenes. Figure 8 shows a schematic representation of the two extreme orientations of a tilted all-*trans* aliphatic chain.

From Figure 7, it can be deduced that ν_s (CH_2) has a preferred orientation nearly parallel to the substrate surface, because it appeared strong in the transmission

(40) Schoondorp, M.; Schouten, A. J.; Hulshof, J. B. E.; Feringa, B. L. *Langmuir* **1992**, *8*, 1852.
(41) Allara, D. L.; Nuzzo, R. G. *Langmuir* **1985**, *1*, 52.
(42) Rabolt, J. F.; Burns, F. C.; Schlotter, N. E.; Swalen, J. D. *J. Electron Spectrosc.* **1983**, *30*, 29.
(43) Allara, D. L.; Swalen, J. D. *J. Phys. Chem.* **1982**, *86*, 2700.
(44) Naselli, C.; Rabolt, J. F.; Swalen, J. D. *J. Chem. Phys.* **1985**, *82*(*4*), 2136.
(45) Duda, G.; Schouten, A. J.; Arndt, T.; Lieser, G.; Smidt, G. F.; Bubeck, C.; Wegner, G. *Thin Solid Films* **1988**, *159*, 221.
(46) Nuzzo, R. G.; Fusco, A.; Allara, D. L. *J. Am. Chem. Soc.* **1987**, *109*, 2358.
(47) Evans, S. D.; Goppert-Berarducci, K. E.; Urankan, E.; Gerenser, L. J.; Ulman, A.; Snyder, R. G. *Langmuir* **1991**, *7*, 2700.
(48) Popovitz-Biro, R.; Hung, D. J.; Shavit, E.; Lahav, M.; Leiserowitz, L. *Thin Solid Films* **1989**, *178*, 203.
(49) Popovitz-Biro, R.; Hill, K.; Shavit, E.; Hung, D. J.; Lahav, M.; Leiserowitz, L.; Sagiv, J.; Hsiung, H.; Meredith, G. R.; Vanherzeele, H. *J. Am. Chem. Soc.* **1990**, *112*, 2498.
(50) Walsh, S. P.; Lando, J. B. *Langmuir* **1994**, *10*, 246.

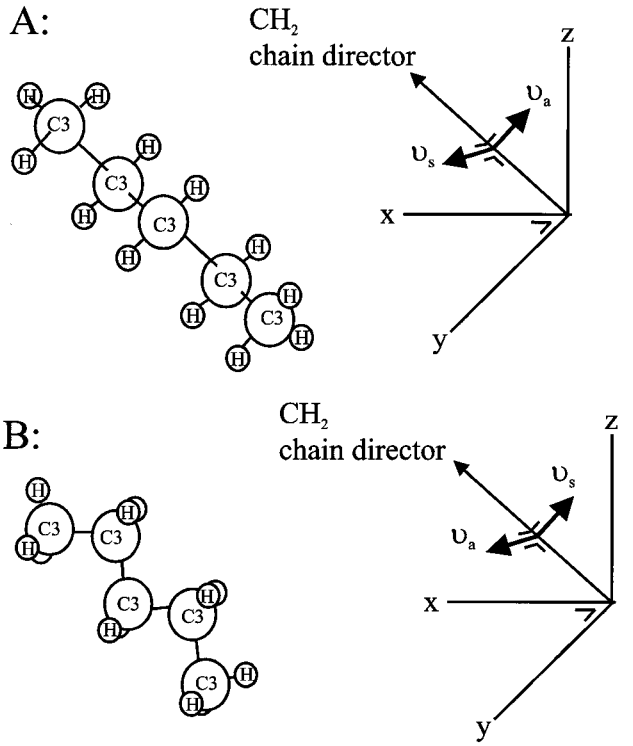

Figure 8. Schematic representation of the two extreme orientations of an all-*trans* aliphatic chain.

spectrum and relatively weak in the GIR spectrum. On the other hand, ν_a (CH_2) vibration was relatively strong in the GIR spectrum compared with the ν_s (CH_2) vibration in this spectrum. However, the absolute value of the ν_a (CH_2) vibration in the GIR spectrum is smaller compared with the transmission and bulk spectrum, indicating a large tilt angle (α) of the chain director with respect to the surface normal. So, Figure 8A represents the suggested situation in which the transition dipole moment of the ν_s (CH_2) vibration is parallel to the substrate surface and the transition dipole of the ν_a (CH_2) vibration has a considerable component perpendicular to the substrate surface.

From the results obtained from the small-angle X-ray reflection measurements together with the result from the FT-IR spectra we propose a model for the multilayer film (Figure 9) built up from a 5 mM $Cu(ClO_4)_2$ subphase, where α is the tilt angle relative to the surface normal and β is the rotation about the molecular axis compared with the structure in Figure 8B. From the experimental data, a value of 35° was found for α, taking into account a bilayer spacing of 59.2 Å and a large tilt angle of the aliphatic tail as is deduced from the IR spectra, which is not unusual for diacetylenes, where normally values between 20 and 45° are found[51] and β should be nearly 90°[47] because ν_s (CH_2) can hardly be observed in the GIR spectrum.

When the subphase contained 5 mM $CuCl_2$, monolayers could only be transferred onto silicon or glass substrates and not onto gold substrates, so only transmission IR spectra could be recorded. These spectra (not shown here) closely resemble the transmission spectra of multilayers built up from a 5mM $Cu(ClO_4)_2$ subphase. Furthermore, the multilayers built up from both subphases have nearly the same bilayer spacing as was derived from the small-angle X-ray reflection measurements; so, it was assumed the multilayers built up from both subphases have nearly the same structure.

(51) Tieke, B.; Lieser, G.; Weiss, K. *Thin Solid Films* **1983**, *99*, 95.

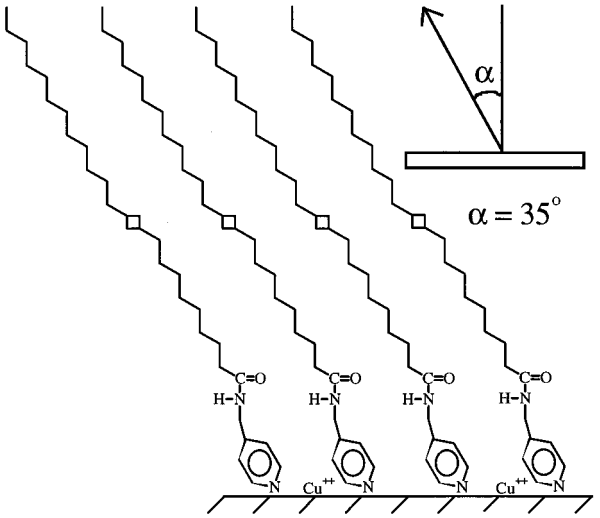

Figure 9. Schematic representation of the structure of amphiphiles inside the multilayers.

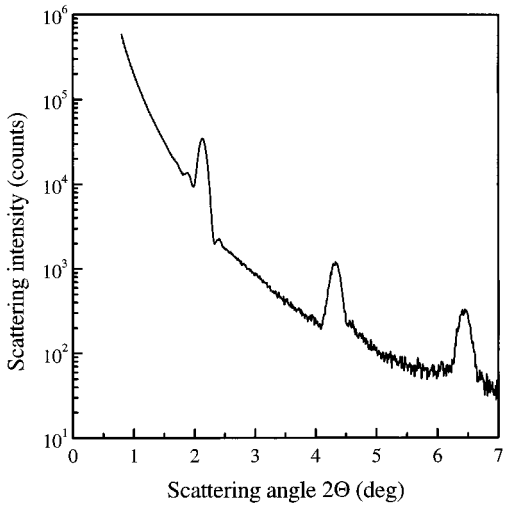

Figure 10. Small-angle X-ray reflection curve of an LB film consisting of 16 layers of the amphiphile on silicon, built up from a 5 mM $CdBr_2$ subphase (sample F) at 19 °C and 19 mN m^{-1}.

Cd(II)-Containing Multilayers. Multilayers could also be built up from a 5mM $CdBr_2$ subphase by Z-type transfer at a subphase temperature of 20 °C and surface pressures between 15 and 20 mN m^{-1}. XPS measurements were performed for a direct observation of Cd(II) ions in these LB films. The Cd(II) peaks can be seen clearly at ~405 ($3d_5$) and 412 ($3d_3$) eV.[52] The amount of Cd(II) ions incorporated is ~1 Cd(II) ion to two amphiphiles, as calculated from the ratio Cd(II) to N.

Small-angle X-ray reflection measurements (Figure 10), showed a regular layer structure with a layer spacing of ~42 Å. This result might be ascribed to a monolayer spacing, assuming that the amphiphiles are oriented perfectly perpendicular to the substrate (α = 0°) or it represents a bilayer spacing with a very large tilt angle, α, of the chain director with respect to the surface normal.

In Figure 11, the transmission IR spectrum of sample F can be seen. It appeared to be impossible to transfer monolayers onto gold- or silver-coated glass substrates even when these substrates were covered first with five layers cadmium arachidate or four layers of amylose-

(52) Briggs, D., Seah, M. P., Ed.; *Practical Surface Analysis*; John Wiley & Sons: Chichester and New York, 1984.

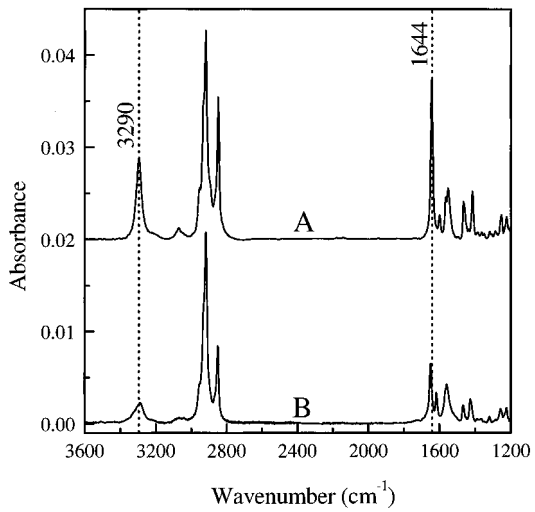

Figure 11. Infrared spectra of the amphiphile: (A) bulk spectrum of the amphiphile, powdered in KBr (scale factor: 0.0395×); (B) transmission, 16 layers of the amphiphile on silicon built up from a 5 mM $CdBr_2$ subphase (sample E) at 19 °C and 19 mN m^{-1}.

acetate[40] or poly((*S*)-1-acetoxymethylethyl-isocyanide);[53] so, GIR spectra could not be recorded.

For the bulk spectrum, the same scaling factor was used as in Figure 7. In the transmission spectrum (Figure 11B), the N−H (3290 cm^{-1}) and amide I (1644 cm^{-1}) absorption bands can clearly be seen, but their relative intensity is weaker than in the bulk spectrum, indicating that the amide bond has a large tilt angle with respect to the surface normal. Also, the aliphatic tail vibrations [2920 cm^{-1} for ν_a (CH_2) and 2850 ν_s (CH_2)] should have a much stronger absorption in the transmission spectrum when the aliphatic tails were oriented almost perpendicular to the substrate. However, from Figure 11 it can be concluded that the aliphatic tail has a large tilt angle (α) with respect to the substrate surface. The carbon−nitrogen stretch vibration absorption is present at 1618 cm^{-1}, indicating that the Cd(II) ions are indeed coordinated to the pyridine ring of the amphiphile.

The transmission spectrum suggest a large tilt angle (α); so, from the IR spectrum it can be concluded that the spacing of 42 Å represents a bilayer spacing. Again a "turnover" from a Z-type structure to a Y-type structure must have occurred because these multilayers were also built up with a Z-type transfer. From these results we propose a structure for the multilayer that deviates a little from the LB film built up from a Cu(II) subphase. The tilt angle (α) of the chain director with the surface normal is ∼55°.

So, when the multilayers contain Cd(II) ions, the amphiphiles have a larger tilt angle with respect to the surface normal than in the case when the multilayers contain Cu(II) ions.

Polymerization in the Multilayers. The LB film were polymerized by exposure to UV light (λ = 254 nm) under argon atmosphere. The polymerization process was followed by UV−vis spectroscopy. Figure 12A exhibits absorption spectrum changes during the UV irradiation of the LB film consisting of 16 layers, built up from a 5 mM $Cu(ClO_4)_2$ subphase. Several minutes of exposure to UV light resulted in a red form of the polymer with λ_{max} = 540 nm. So, upon UV irradiation, a rigid polymer with a one-dimensional conjugated backbone is formed. The

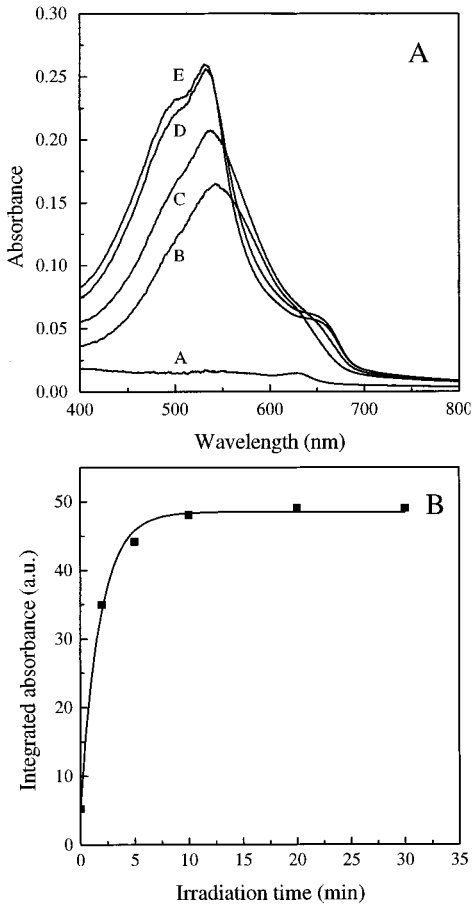

Figure 12. A. UV−vis spectra of an LB film of 16 layers of the amphiphile built up from a 5 mM $Cu(ClO_4)_2$ subphase (sample B) at 19 °C and 30 mN m^{-1} on glass, at different UV (λ = 254 nm) irradiation times: (A) 0 min, (B) 2 min, (C) 5 min, (D) 20 min, and (E) 30 min. (B) Integrated absorbance from the UV−vis spectra of Figure 11A, between 400 and 800 nm, at different times of exposure to UV light.

conjugation resulted in the strong π to π^* absorption[54,55] shown in Figure 12A. In Figure 12B, the integrated area of absorbance between 400 and 800 nm is shown. Apparently, the polymerization is complete after 20 min of exposure to UV light. The optical density at 540 nm is ∼0.008 per diacetylene monolayer. This is about the maximum obtainable optical density for a polydiacatylene monolayer.[24] So, the polymerization was more or less complete after 20 min of UV irradiation. In the case of the multilayers built up from a 5 mM $CuCl_2$ subphase, however, the polymerization was complete only after ∼50 min of exposure to UV light. Thus, by changing the counterion, the polymerization properties can be influenced, probably caused by a slightly different packing of the monomers. The polymerization of diacetylenes is a topochemical reaction, so, a slightly different packing of the amphiphiles can have an enormous influence on the polymerization behavior.[56]

Upon exposure to UV light no reduction of the Cu(II) ions inside the LB films to Cu(I) ions has been observed because the copper(II) peaks at 936.5 and 956.5 eV with their corresponding satellite peaks could clearly be seen in the XPS spectrum of these films after exposure to UV light.

(53) Teerenstra, M.; Vorenkamp, E. J.; Nolte, R. J. M.; Schouten, A. J. *Thin Solid Films* **1991**, *196*, 153.

(54) Deckert, A. A. D.; Fallon, L.; Kiernan, L.; Cashin, C.; Perrone, A.; Encalarde, T. *Langmuir* **1994**, *10*, 1948.

(55) Deckert, A. A.; Horne, J. H. C.; Valentine, B.; Kiernan, I.; Fallon, L. *Langmuir* **1995**, *11*, 643.

(56) Tieke, B. *Adv. Poly. Sci.* **1985**, *71*, 79.

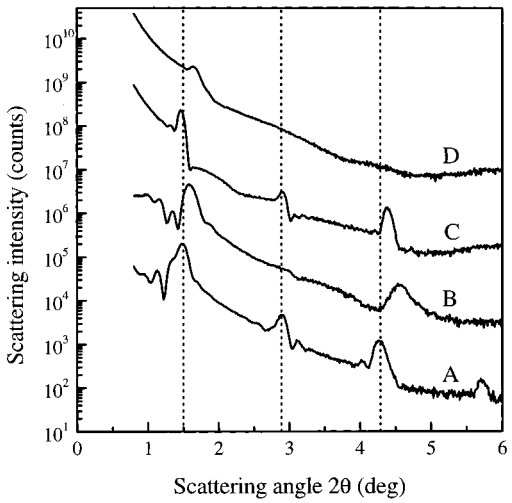

Figure 13. Small-angle X-ray reflection curves of an LB film of 16 layers of the amphiphile built up from a 5 mM $Cu(ClO_4)_2$ subphase (sample A) at 19 °C and 30 mN m^{-1} on silicon, before (A) and after (B) 20 min of UV irradiation, and small-angle X-ray curves of an LB film consisting of 16 layers of amphiphile, built up from a 5 mM $CuCl_2$ subphase (sample E) at 19 °C and 30 mN m^{-1} on silicon, before (C) and after (D) 50 min of exposure to UV light.

To examine whether the regular layer pattern was preserved during the polymerization process, small-angle X-ray reflection measurements were performed. In Figure 13(A and B), small-angle x-ray reflection measurements of sample A are shown (subphase: 5 mM $Cu(ClO_4)_2$) before and after 30 min of UV irradiation. From these measurements it can be concluded that the layer structure is preserved during UV irradiation, although the bilayer spacing decreased from 59.2 down to 57.4 Å and the second-order Bragg peak disappeared. The latter phenomenon can be explained by means of the well-known odd−even intensity oscillations of X-ray diffraction profiles.[57−60] In Y-type multilayer films, the juxtaposition of the two hydrophobic ends of the amphiphiles can give rise to a electron-deficient layer that will influence the intensity of the diffraction peaks. By variation of the layer thickness of this electron-deficient layer, the intensities of the diffraction peaks can be varied, which was already shown in 1977 by Matsuda et al.,[57] who found that the best agreement between the calculated and experimental diffraction patterns for LB films of cadmium salts of fatty acids was found when an electron-deficient layer of about two CH_2 groups thick was taken into account. As we can see from Figures 6A and 13A, already before exposure to UV light the second Bragg peak had a relatively weaker intensity than the third one, which is additional proof of the existence of a Y-type structure in the LB film.[60] The shift of the Bragg peak to higher angles indicates an increased tilt of the amphiphiles inside the multilayer.

Contrary to LB films prepared from a $Cu(ClO_4)_2$-containing subphase, the layer structure of the LB film built up from a $CuCl_2$ subphase was destroyed after exposure to UV light, which is clearly demonstrated in Figure 13 (curves C and D).

To get more insight in the structural changes inside the multilayer during the polymerization process, FT-IR spectroscopy measurements were performed. During the exposure to UV light, the major changes were found in the CH stretching region, for multilayers built up from a 5 mM $Cu(ClO_4)_2$ subphase, as can be seen in the Figures 14A (sample C) and B (sample B). The vibration bands near 2850, 2871, 2920, and 2954 cm^{-1} are due to ν_s (CH_2), ν_s (CH_3), ν_a (CH_2), and ν_a (CH_3), respectively.[61,62] The vibration band near 2934 cm^{-1} arises from the Fermi resonance between the ν_a (CH_3) band and the overtone of the CH_3 asymmetric deformation vibration near 1450 cm^{-1}.[61] The weak vibration near 2897 cm^{-1} was assigned to a Fermi resonance component arising from the ν_s (CH_2) band and an overtone of the CH_2 scissoring vibration.[61] After UV irradiation, the ν_s (CH_2) and ν_a (CH_2) bands were slightly shifted to higher frequencies (2852 and 2922 cm^{-1}, respectively). This result indicated that the all-*trans* alkyl chain is partly converted into an alkyl chain containing gauche conformations. Because for an alkyl chain containing all-*trans* conformations, the ν_s (CH_2) and ν_a (CH_2) are situated at 2849 and 2919 cm^{-1}, respectively, whereas for an irregular alkyl chain containing only gauche conformations, these vibrations are situated at 2854 and 2924 cm^{-1}.[61] Furthermore, the ν_s (CH_3) and the ν_a (CH_3)

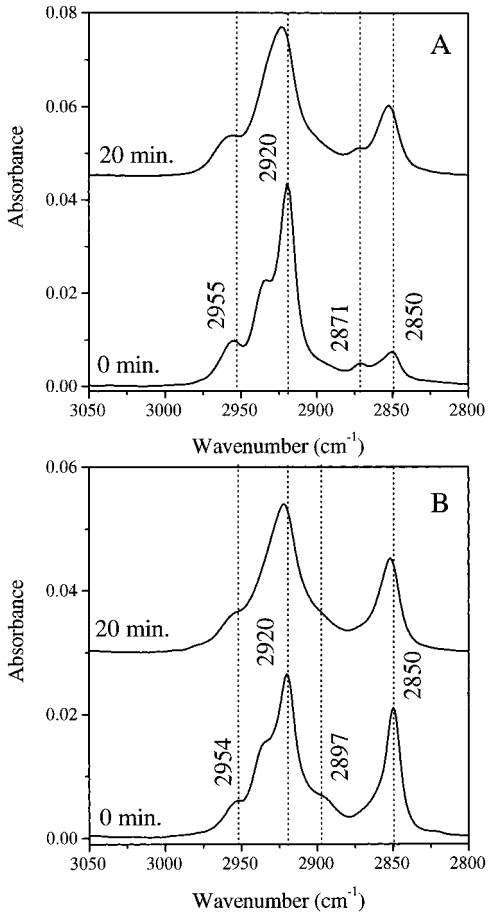

Figure 14. (A) GIR IR spectra of an LB film of 16 layers of the amphiphile built up from a 5 mM $Cu(ClO_4)_2$ subphase (sample C) at 19 °C and 30 mN m^{-1} on gold-coated glass with three layers of cadmium arachidate, before and after 20 min of exposure to UV light. (B) Transmission IR spectra of an LB film of 16 layers of the amphiphile built up from a 5 mM $Cu(ClO_4)_2$ subphase (sample A) at 19 °C and 30 mN m^{-1} on silicon, before and after 20 min of exposure to UV light. The CH_2 and CH_3 stretching vibration region.

(57) Matsuda, A.; Sugi, M.; Fukui, T.; Izima, S.; Miyahara, M.; Otsubo, Y. *J. Appl. Phys.* **1977**, *48(2)*, 771.
(58) Pomerantz, M.; Segmüller, A. *Thin Solid Films* **1980**, *60*, 33.
(59) He, P.; Tian, Q.; Chen, X. *New Polymeric Mater.* **1991**, *3(1)*, 19.
(60) Peltonen, J. P. K.; He, P.; Rosenholm, J. B. *Langmuir* **1993**, *9*, 2363.
(61) Saito, A.; Urai, Y.; Itoh, K. *Langmuir* **1996**, *12*, 3938.
(62) Rabolt, J. F.; Burns, F. C.; Schlotter, N. E.; Swalen, J. D. *Chem. Phys.* **1983**, *78*, 946.

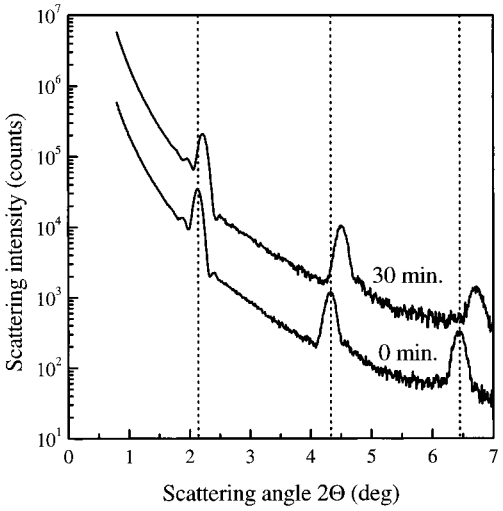

Figure 15. Small-angle X-ray reflection curves of an LB film of 16 layers of the amphiphile built up from a 5 mM $CdBr_2$ subphase (sample F) at 19 °C and 19 mN m^{-1} on silicon, at different times of exposure to UV light.

vibrations are situated at 2871 and 2955 cm^{-1}, respectively, irrespective of the alkyl chain conformation. This result is consistent with our observations. The intensity of the ν_a (CH_2) band decreased in the GIR spectrum whereas the intensity of the ν_s (CH_2) band increased upon UV irradiation (Figure 14A). This fact together with the slight shift of these vibration bands to higher wavenumbers, could be explained by considering that the all-*trans* conformation of the alkyl is converted into an irregular one containing gauche conformations.

The same phenomena appeared in multilayers built up from a 5 mM $CuCl_2$ subphase. But for these multilayers, the intensities of the ν (N−H) and amide I absorptions also decrease in intensity and the peaks become broader, indicating that not only the structure of the aliphatic tail changes upon UV irradiation, but also the amide bond and pyridine rings are reoriented. This result explains why the layer structure almost completely disappeared in the small-angle x-ray measurement (Figure 13, curve D), upon exposure to UV light.

Polymerization of Cd(II)-Containing Multilayers. Upon exposure to UV light (254 nm), the multilayer film built up from a 5 mM $CdBr_2$ subphase formed a red phase polydiacetylene film. The polymerization was complete within 30 min as could be seen by UV−vis spectroscopy, in which the absorption at $\lambda_{max} = 540$ did not increase anymore after 30 min of exposure to UV light.

Small-angle X-ray reflection measurements revealed that the layer structure was preserved well during the UV irradiation (Figure 15). The bilayer spacing decreased from 42 to 40.5 Å, again indicating that upon polymerization the amphiphiles make a larger tilt with respect to the surface normal. We can also observe that the second Bragg peak is present before and after UV irradiation in contrast to the LB films built up from a Cu(II) subphase where the second Bragg peak before UV irradiation was already somewhat weaker in intensity (the well-known odd−even effect) and in the case of ClO_4^- as counterion totally disappeared upon exposure to UV light. This result was a strong indication that the Cu(II) and Cd(II) ions multilayers had different layer structure.

Spectral changes in the transmission IR spectra showed up only in the CH stretching vibration region. The ν_a (CH_2) and ν_s (CH_2) absorptions did not shift to higher wavenumbers as was the case for the Cu(II)-containing multilayers (Figure 14B). So, during the polymerization process, the alkyl chains maintain the all-*trans* conformation. Furthermore, upon polymerization, the ν_a (CH_2) absorption decreases in intensity whereas the ν_s (CH_2) absorption shows a slight increase in intensity. These spectral changes in the transmission spectrum can only be ascribed to a larger tilt angle (α) of the alkyl chain director with respect to the surface normal, which is in good agreement with the observed decrease in bilayer spacing derived from the small-angle x-ray measurements (Figure 15).

Conclusions

The LB multilayers of 4-(10,12-pentacosadiynamidomethyl)pyridine could only be built up when the subphase contained Cu(II) or Cd(II) ions. The XPS measurements confirmed that complexation had occurred in the monolayer because the multilayers contained metal ions. Care must be taken in drawing conclusions about the valence of the copper ions inside these multilayers from data deduced by XPS measurements, because upon exposure to X-rays, the Cu(II) ions undergo a X-ray-induced reduction to Cu(I). Small-angle X-ray reflection measurements revealed that the formed multilayers had a regular layer structure with a bilayer spacing of ∼60 Å and ∼42 Å for the Cu(II) ion- and Cd(II) ion-containing multilayers, respectively, although these multilayers were built up by a Z-type transfer. So, a rearrangement to a Y-type structure had occurred.

Changes of metal ion had a great effect on the structure and polymerization properties of these multilayers. Multilayers built up from $Cu(ClO_4)_2$- and $CdBr_2$-containing subphases preserve their regular layer structure during the polymerization process. But after polymerization, the all-*trans* alkyl of the amphiphile in a Cu(II) ion-containing multilayer is converted into a more irregular alkyl chain containing gauche conformations. This result did not occur in the Cd(II)-containing multilayers. For LB films built up from a $CuCl_2$ subphase, the regular layer structure was not preserved during the polymerization process.

To summarize, the properties of LB film of metal complexes largely depend on the metal and counterions used in the subphase, from which the multilayers are built up.

LA9706429